Design of a High-Gain Single-Feed Quad-Beam Metalens with Polarization Conversion at 0.1 THz

Xuekang Liu[1], Daniel Rodriguez Prado[1], Claudio Paoloni[1], Rosa Letizia[1], Lu Zhang[2], Benito Sanz-Izquierdo[3], Steven Gao[4], Lei Wang[1]

[1] (Lancaster University): School of Engineering, Lancaster, UK, xuekangliu@ieee.org

[2] (Swansea University): Faculty of Science and Engineering, Swansea, UK.

[3] (University of Kent): School of Engineering, Canterbury, UK.

[4] (Chinese University of Hong Kong): Department of Electronic Engineering, Hong Kong, China

***Abstract*—This paper presents a novel 2-bit single-feed quad-beam metalens antenna for sub-THz links powered by traveling wave tubes. The metalens surface, consisting of 7692 unit cells with orthogonal slots and vias, allows precise electromagnetic wave manipulation by adjusting slot lengths to control the transmission phase. Rotating the lower-layer slots in opposite directions creates a stable 180° phase difference, providing over 530° phase coverage. The design is fed by a custom pyramid horn with a WR-10 waveguide interface, optimized for single-unit fabrication. The superposition method was used to achieve the required phase distribution, generating four beams at φ = (0°, 90°, 180°, 270°) and θ = 15°, with a peak gain of 32.28 dBi at 106 GHz and all beams above 30.15 dBi within 102-109.5 GHz. This high-performance metalens offers a promising solution for future 6G high-capacity links.**

***Index Terms*— Sub-THz communication, Metalens, Quad Beam, High Gain, 6G**

I. INTRODUCTION

The advancement of wireless communication systems has accelerated with the advent of fifth generation (5G) networks, but the increasing demand for higher data rates, lower latency, and more efficient spectrum use has pushed research towards the development of sixth generation (6G) communication systems. One of the key enablers of 6G is the utilization of frequencies in the sub-terahertz (sub-THz) band, particularly the W-band in the 102-109.5 GHz range [1], which offers a wide bandwidth and the potential for ultra-high data rates with tens of Gb/s. These characteristics are essential for supporting data-intensive applications like high capacity backhaul for high density cells.

In this frequency range, the high free-space loss [2] and the attenuation caused by rain and atmospheric gases present significant challenges, requiring the use of very high-gain antennas due to the limited power output of solid-state power amplifiers (SSPAs). However, the development of a new generation of traveling wave tubes (TWTs) [3], [4] at sub-THz frequencies will deliver transmission power more than two orders of magnitude higher, enabling reliable links with compact, relatively high-gain antennas for both single and multi-beam data distribution.

Metalenses (metasurface lenses) [5], [6], [7] offer a promising solution to achieve the required high-gain performance with precise control of electromagnetic waves. These devices leverage artificially structured materials to manipulate the phase, or both amplitude and phase, at sub-wavelength scales, enabling the formation of highly directional beams. This precise wavefront shaping makes metalenses ideal for use in sub-THz applications in 6G communication systems.

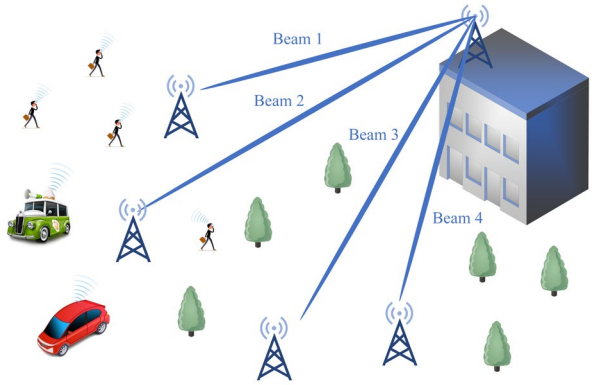

Fig. 1. Application scenarios of multi-beam sub-THz metalens.

As is illustrated in Fig.1, multi-beam metalenses further extend these capabilities by enabling multiple simultaneous data streams through multiple distinct beams, with adequate transmission power (about 40 dBm) provided by a W-band TWT. This improves the coverage, reduces the equipment footprint, improves spectral efficiency and network capacity, which are critical for 6G networks such as backhaul links. Although several multi-beam designs [8], [9], [10] have been reported, most of these are designed to operate at lower frequency bands. To date, very few multi-beam metalens based on standard PCB technology operating above 100 GHz have been reported [11], highlighting the urgent need to design a suitable solution for such high-frequency applications.

In this paper, we present the design and analysis of a high-gain single-feed quad-beam metalens with polarization conversion operating in the 102-109.5 GHz frequency band to be integrated with a TWT amplifier [12] for enabling long-range multi-beam sub-THz links. The unit cells are realized using orthogonal slot structure, where the transmission phase

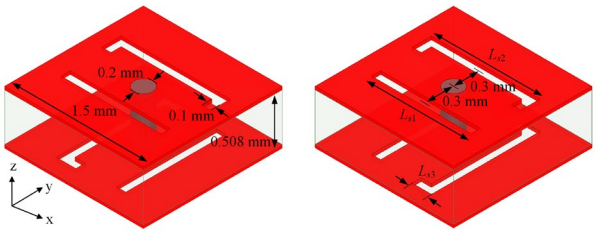

(a) (b)

Fig. 2. Geometry of the (a) unit cell 1 and (b) unit cell 2 with 180° phase difference.

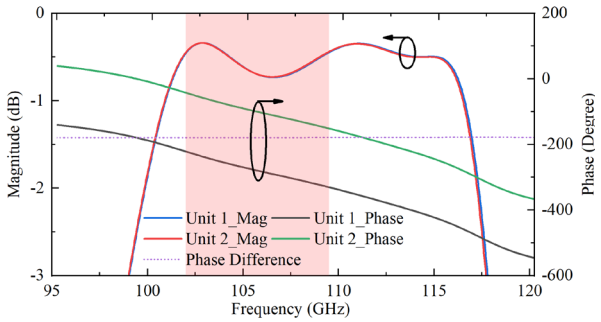

Fig. 3. Transmission coefficients and phases of the unit cell 1 and 2.

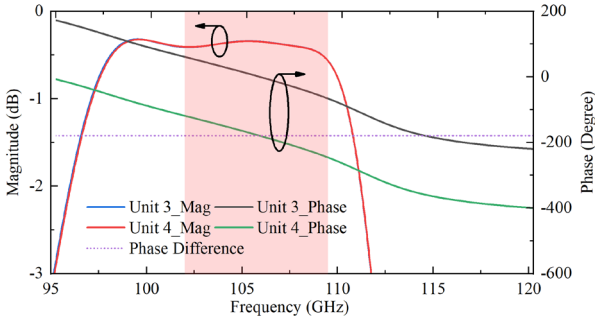

Fig. 4. Transmission coefficients and phases of the unit cell 3 and 4.

TABLE I
KEY PARAMETERS

Unit Cell	L_{s1} (mm)	L_{s2} (mm)	L_{s3} (mm)
#1	1.08	1.18	0.21
#2	1.08	1.18	0.21
#3	1.16	1.20	0.25
#4	1.16	1.20	0.25

is controlled by adjusting slot lengths. To enhance gain bandwidth, multiple slots of varying lengths are employed. Using the superposition method, a four-beam metalens is achieved, fed by a pyramid horn connected to a WR-10 waveguide.

II. UNIT CELL DESIGN

In this design, two groups of multi-slot unit cells are used to achieve 360° coverage. Group 1 consists of unit cells 1 and 2, which are illustrated in Fig. 2. Group 2 comprises unit cells 3 and 4. Since the only difference between unit cell 1 and unit cell 3, and between unit cell 2 and unit cell 4, is the length of the slots, only the geometries of unit cells 1 and 2 are provided here for reference. As observed, unit cell 1 consists of two metal layers and a substrate layer. The substrate used has a dielectric constant of 2.2 and a loss tangent of 0.0009. The slots on both the upper and lower metal layers share the same structure but are rotated by 90°. As described in [13], the slot array behaves as a band-pass surface, where only specific polarizations of EM (electromagnetic) waves can pass. Thus, without the introduction of vias, the metal layers would reflect most of the electromagnetic waves with any polarization, severely limiting the transmission efficiency. The vias play a crucial role in enhancing the slot surfaces' performance by facilitating the passage of specific polarized electromagnetic waves, significantly improving transmission efficiency and reducing unwanted reflections between the metal layers [14]. Additionally, in this case, the polarization of the incident wave is converted into its orthogonal polarization.

Unit cell 2 has the same dimensions as unit cell 1, with the key difference being the rotation method of the slots on the lower metal layer. In unit cell 1, the slots on the bottom layer are rotated 90° relative to the upper layer. However, in unit cell 2, the bottom slots are rotated -90°. This opposing rotation enables the two unit cells to maintain a stable 180° phase difference, crucial for achieving consistent performance in the design. The simulated transmission coefficients, transmission phases, and phase differences for the unit cells in group 1 are shown in Fig. 3. As observed, the unit cells achieve identical transmission coefficients and maintain a stable 180° phase difference, which meets the design requirements for consistent and reliable performance. The same characteristics are observed in the unit cells (unit cell 3 and 4) of group 2, as illustrated in Fig. 4.

Based on these two groups of unit cells, a 360° phase range can be covered by a quantized 2-bit phase distribution (90°, 180°, 270°, 360°), ensuring effective phase control and coverage. Considering the constraints of PCB technology, the final key parameters of the four unit cells are given in Table I. All other parameters are given in Fig. 2.

III. QUAD-BEAM METALENS DESIGN

As stated in [8], there are two primary methods for designing multi-beam metalenses. The first is a geometrical approach, which involves dividing the entire surface into M sub-arrays, with each sub-array radiating a beam in the desired direction. While this method simplifies the design process, it significantly reduces the metalens's gain, as each beam is generated by only a fraction ($1/M$) of the total array aperture, limiting overall performance.

Another approach is known as the superposition method. In this method, the phase distribution for each of the four beams is calculated individually, and the total phase distribution is obtained through the superposition of these

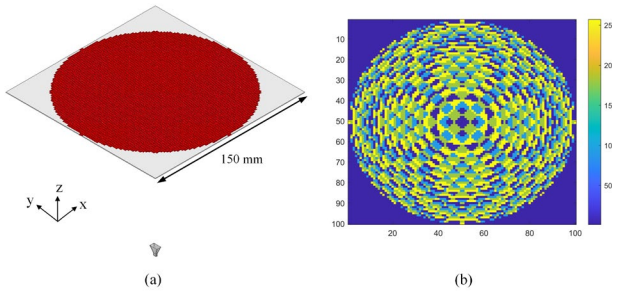

Fig. 5. (a) Configuration and (b) calculated phase distribution of the quad-beam meta-lens.

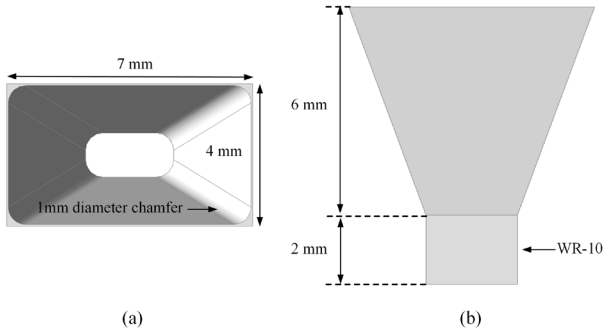

Fig. 6. (a) Top view and (b) side view of the proposed horn.

phases. This technique not only generates multiple beams in different directions but also ensures that each beam is formed by the combined electromagnetic fields from the entire array, leading to higher gain. The design presented in this article is based on this superposition method.

To generate M beams with a single feed, the tangential field on the metalens surface can simply be written as:

$$E(x_i, y_i) = \sum_{m=1}^{M} A_m(x_i, y_i) e^{j\emptyset_{m(x_i,y_i)}} \quad (1)$$

where (x_i, y_i) represents the position of the elements, while A_m and $\emptyset_m$ denote the amplitude and phase needed to generate the m_{th} beam in (θ_m, φ_m) direction. However, the amplitude at each element is imposed by the feed, so only the phase distribution is considered for generating the desired beams. The phase shift required for each beam at each element is calculated as follows:

$$\emptyset_{m(x_i,y_i)} = -k_0 sin\theta_m (cos\varphi_m x_i + sin\varphi_m xy_i) \quad (2)$$

By superimposing the required electric fields for each of the four beams, the phase distribution for the array, capable of generating all four beams, can be obtained. But it should be noted that the final phase distribution should also include the phase compensation for each unit by using:

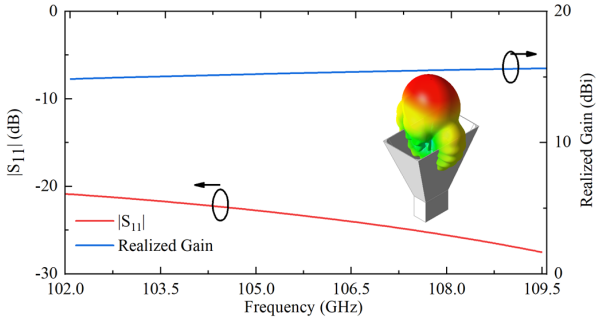

Fig. 7. Simulated $|S_{11}|$ and realized gain in broadside direction of the horn.

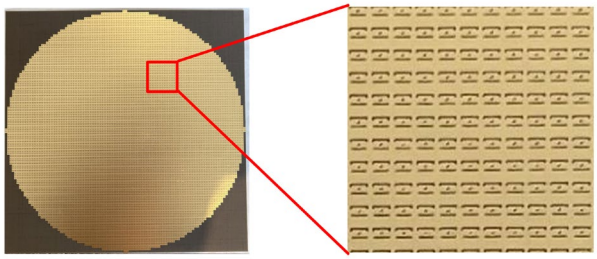

Fig. 8. Photo of the prototype.

$$k_0 \times (r_{mn} - r_0) + \varphi_{mn} = 2n\pi, n = 0, \pm 1, \ldots, \quad (3)$$

In this context, k_0 represents the wavenumber in free space, while r_{mn} is the distance between the phase center of the horn and the i_{th} element. r_0 refers to the distance between the phase center of the horn and the center of the metalens. φ_{mn} is the compensation phase of the i_{th} element.

The configuration and the required phase distribution of a 7692 elements circular metalens is given in Fig. 5. The distance between the metalens surface and the horn phase center is 135 mm, which corresponds to 0.9 times the substrate length (150 mm). The feed source is a custom-designed pyramid horn. To account for CNC (Computer Numerical Control) machining limitations for fabricating the horn as a single unit, specific modifications were made. As shown in Fig. 6, the horn's WR-10 waveguide interface and the flare's four corners were chamfered for easier machining. Since the horn will be manufactured as a single piece using Lancaster University's CNC equipment, the total antenna length, including the waveguide section, is restricted to 8 mm to meet machining constraints. As depicted in Fig. 7, the $|S_{11}|$ of the proposed horn remains below -20 dB across the target frequency range, ensuring good impedance matching. The realized gain exceeds 14.76 dBi within the same range. At 106 GHz, the half-power beamwidths (HPBW) are 36.59° in the E-plane and 27.54° in the H-plane.

IV. Results

To validate the design concept, the proposed metalens was fabricated, and the prototype is shown in Fig. 8. However, an unforeseen mechanical issue prevented the completion of the

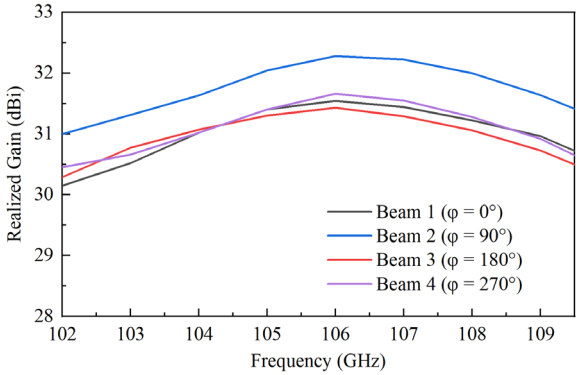

Fig. 9. Peak realized gains of each beam of the quad-beam metalens varies with frequency.

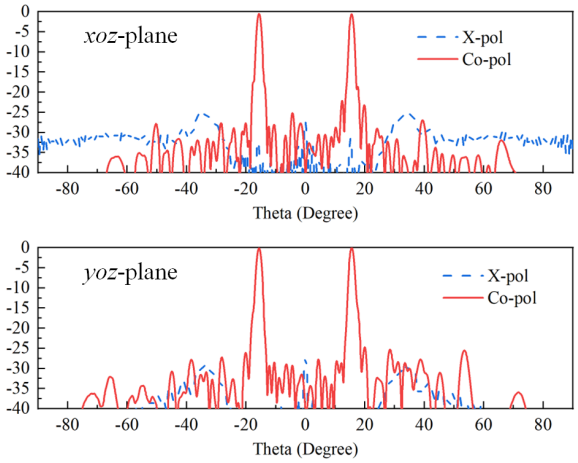

Fig. 10. Normalized radiation patterns of the quad-beam metalens at 102 GHz.

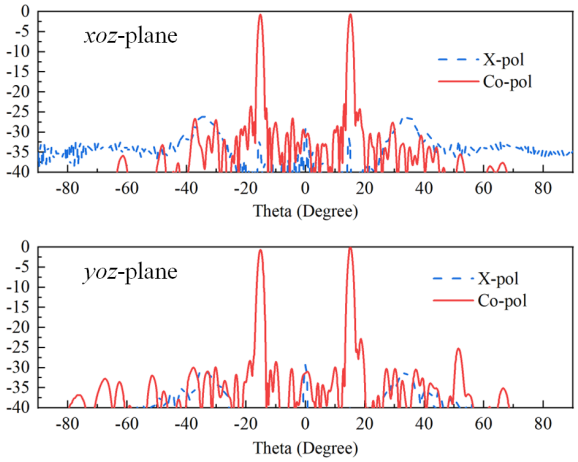

Fig. 11. Normalized radiation patterns of the quad-beam metalens at 105 GHz.

testing as initially planned. Consequently, only simulated results are presented here.

Fig. 9 illustrates the peak realized gains of each beam of the proposed metalens at various frequencies. The results

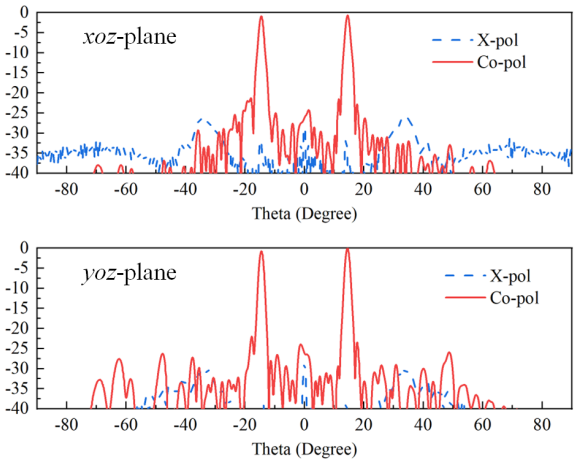

Fig. 12. Normalized radiation patterns of the quad-beam metalens at 109.5 GHz.

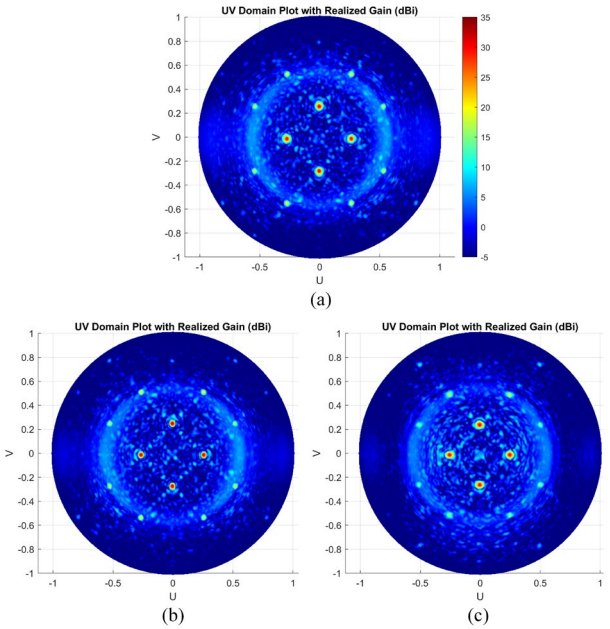

Fig. 13. UV domain plot at (a) 102 GHz, (b) 105 GHz, and (c) 109.5 GHz.

show that the proposed design achieves a gain higher than 30.15 dBi across the target frequency range (102-109.5 GHz), with a peak gain of 32.28 dBi at 106 GHz. Figs. 10, 11, and 12 present the normalized radiation patterns at 102 GHz, 105 GHz, and 109.5 GHz, respectively. As shown, four beams are successfully generated, each pointing in the target directions ($\varphi = 0°, 90°, 180°, 270°$ and $\theta = 15°$).

It is important to note that, theoretically, using the superposition method allows us to generate any number of beams in any direction. In this paper, we selected these specific values to validate the design approach. The sidelobe levels are at least 20 dB lower than the main beams in both the xoz and yoz planes. The half-power beamwidths are $1.37° \pm 0.7°$ in the xoz-plane and $1.46° \pm 0.4°$ in the yoz-plane. Overall, these results demonstrate that the proposed design

exhibits stable radiation performance. The UV domain plots are presented in Fig. 13, where the UV grid is defined as $u = \sin\theta\cos\phi$ and $v = \sin\theta\sin\phi$, with θ and ϕ representing the standard spherical coordinates in the far field. As can be observed, most of the energy is effectively concentrated in the four main beam areas, which is crucial for efficient signal transmission. This is especially important in the sub-THz band, where free-space path loss is significant, making focused beam control essential for maintaining signal strength and reducing power loss. In applications requiring high-directionality and minimal interference, such beam concentration ensures better performance and reliability, especially in long-range communication or sensing systems operating in high-frequency ranges.

V. CONCLUSION

In this paper, we have developed a high-gain 2-bit single-feed quad-beam metalens with polarization conversion for sub-THz high capacity links. The metalens consists of 7692 unit cells, featuring orthogonal slot structures and vias to achieve precise phase control. Two groups of unit cells with a stable 180° phase difference were used to provide full 360° phase coverage. By applying the superposition method, the metalens successfully generated four distinct beams with gains exceeding 30.15 dBi across the 102–109.5 GHz range, peaking at 32.28 dBi at 106 GHz. These results highlight the effectiveness of the unit cell design and the metalens' ability to address key challenges in sub-THz communications, particularly for multi-beam system powered by TWTs.

ACKNOWLEDGMENT

This work is partially supported by the Innovate UK SBRI: Future Telecommunications Challenges No. 10102343, the Engineering and Physical Sciences Research Council (EPSRC) under Grant EP/Y003144/2, the Research Grants Council of Hong Kong through Grants GRF 14210623 and AoE/E-101/23-N, and the PoC project (2324-01-11) funded by the University of Hertfordshire.

REFERENCES

[1] ITU Defines Frequency Bands for 6G Studies. Accessed: Oct. 2024. [online]. Available: https://www.6gworld.com/exclusives/itu-defines-frequency-bands-for-6g-studies/.

[2] T. S. Rappaport et al., "Wireless communications and applications above 100 GHz: Opportunities and challenges for 6G and beyond," *IEEE Access*, vol. 7, pp. 78729–78757, 2019.

[3] C. Paoloni, "Sub-THz wireless transport layer for ubiquitous high data rate," *IEEE Commun. Mag.*, vol. 59, no. 5, pp. 102–107, 2021.

[4] C. Paoloni and et al., "Millimeter wave traveling wave tubes for the 21st century," Journal of Electromagnetic Waves and Applications, vol. 35, no. 5, pp. 567–603, 2020.

[5] Q. Lou and Z. N. Chen, "Sidelobe suppression of metalens antenna by amplitude and phase controllable metasurfaces," *IEEE Trans. Antennas Propag.*, vol. 69, no. 10, pp. 6977-6981, Oct. 2021.

[6] F. F. Manzillo, A. Clemente, and J. L. González-Jiménez, "High-gain D -band transmitarrays in standard PCB technology for beyond-5G communications," *IEEE Trans. Antennas Propag.*, vol. 68, no. 1, pp. 587–592, Jan. 2020.

[7] A. H. Abdelrahman, A. Z. Elsherbeni, and F. Yang, "High-gain and broadband transmitarray antenna using triple-layer spiral dipole elements," *IEEE Antennas Wireless Propag. Lett.*, vol. 13, pp. 1288–1291, 2014.

[8] P. Nayeri, F. Yang, and A. Z. Elsherbeni, "Design and experiment of a single-feed quad-beam reflectarray antenna," *IEEE Trans. Antennas Propag.*, vol. 60, no. 2, pp. 1166–1171, Feb. 2012.

[9] H.-X. Xu, T. Cai, Y.-Q. Zhuang, Q. Peng, G.-M. Wang, and J.- G. Liang, "Dual-mode transmissive metasurface and its applications in multibeam transmitarray," *IEEE Trans. Antennas Propag.*, vol. 65, no. 4, pp. 1797-1806, Feb. 2017.

[10] Z. H. Jiang, L. Kang, T. Yue, W. Hong, and D. H. Werner, "Wideband transmit arrays based on anisotropic impedance surfaces for circularly polarized single-feed multibeam generation in the Q-band," *IEEE Trans. Antennas Propag.*, vol. 68, no. 1, pp. 217-229, Jan. 2020.

[11] Y. J. Guo et al., "Quasi-optical multi-beam antenna technologies for B5G and 6G mmWave and THz networks: A review," *IEEE Open J. Antennas Propag.*, vol. 2, pp. 807–830, 2021.

[12] F. Andre, J.-C. Racamier, R. Zimmermann, Q. Trung Le, V. Krozer, G. Ulisse, D. F. G. Minenna, R. Letizia, and C. Paoloni. Technology, assembly, and test of a W-band Traveling Wave Tube for new 5G high-capacity networks. *IEEE Trans. Electron Devices*, vol. 67, no. 7, pp. 2919–2924, July, 2020.

[13] B. A. Munk, *Frequency Selective Surfaces: Theory and Design*. New York, NY, USA: Wiley-Interscience, 2000.

[14] W. Hu et al., "A wideband metal-only transmitarray with two-layer configuration," *IEEE Antennas Wireless Propag. Lett.*, vol. 20, no. 7, pp. 1347–1351, Jul. 2021.